

Electronic Supplementary Material (ESI) for Nanoscale Advances. This journal is ©
The Royal Society of Chemistry 2021

Supporting Information

Dual-regulating Strategy Fabrication of Porous NiFeP/Ni Electrode for Highly Efficient Hydrazine Oxidation Boost H₂ Evolution

Honglei Wang, Shengyang Tao*

Department of Chemistry, School of Chemical Engineering, Dalian University of
Technology, Dalian 116024, China.

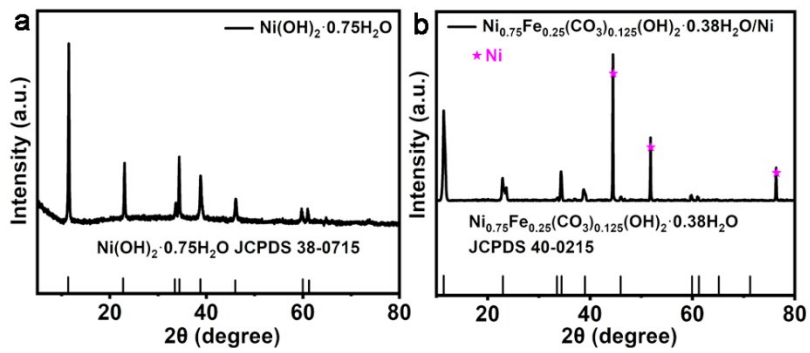


Fig. S1 (a) The XRD patterns of $\text{Ni}(\text{OH})_2 \cdot 0.75\text{H}_2\text{O}$ and (b) Pre-NiFe/Ni.

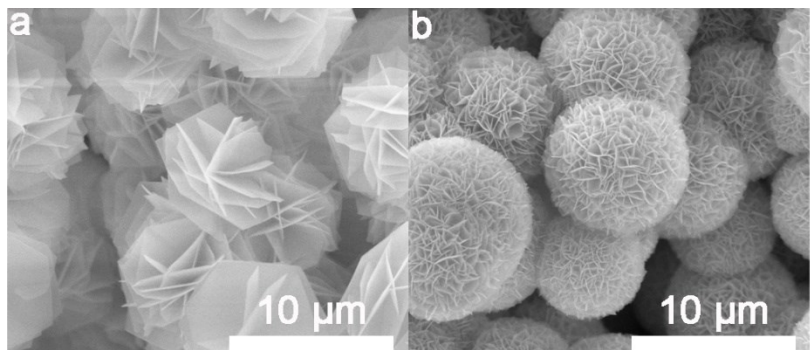


Fig. S2 (a) The SEM images of $\text{Ni}(\text{OH})_2 \cdot 0.75\text{H}_2\text{O}/\text{Ni}$ and (b) Pre-NiFe/Ni.

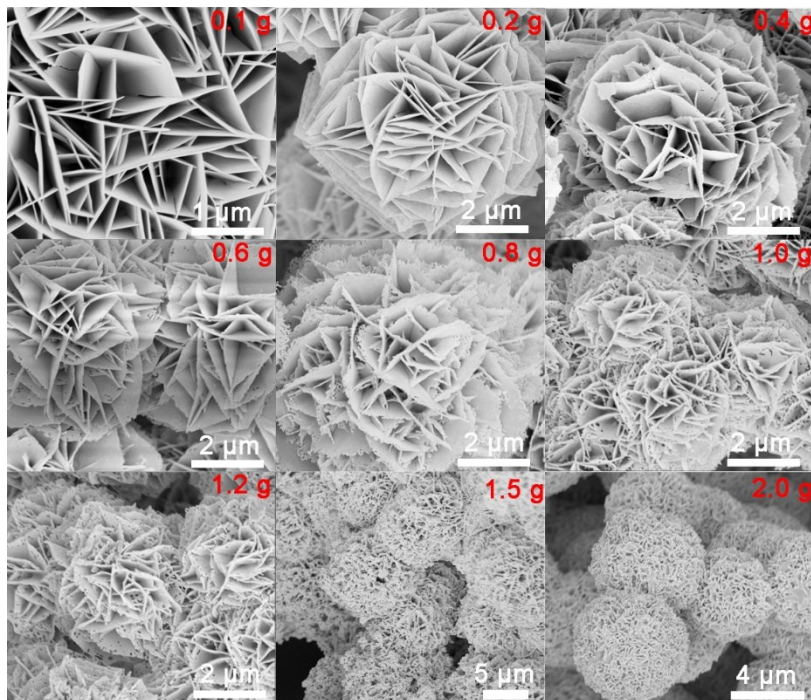


Fig. S3 The SEM images of P-NiFeP/Ni under the different phosphorus sources content.

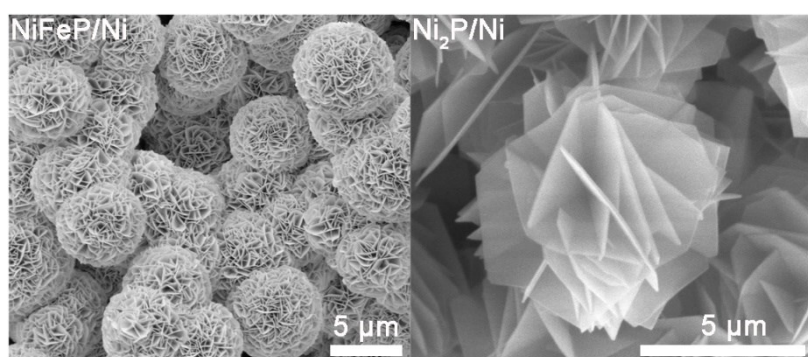


Fig. S4 The SEM images of NiFeP/Ni and Ni₂P/Ni under the same phosphating conditions as P-NiFeP/Ni.

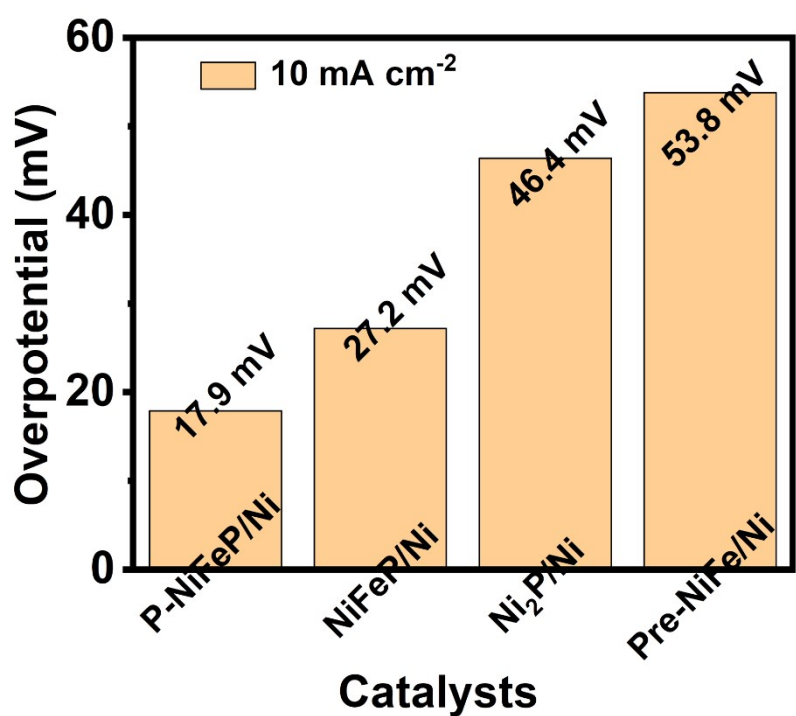


Fig. S5 The overpotential of the catalysts at 10 mA cm^{-2} .

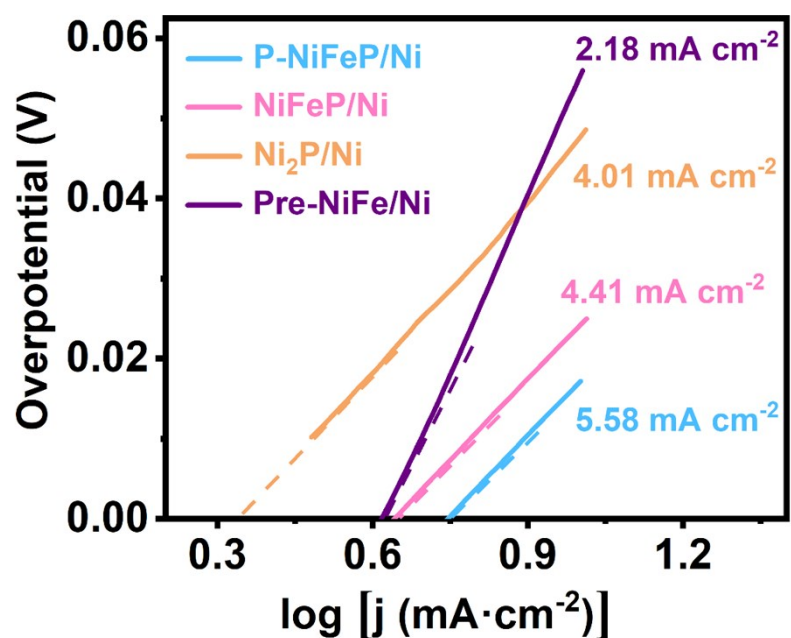


Fig. S6 The exchange current density of the as-prepared catalysts.

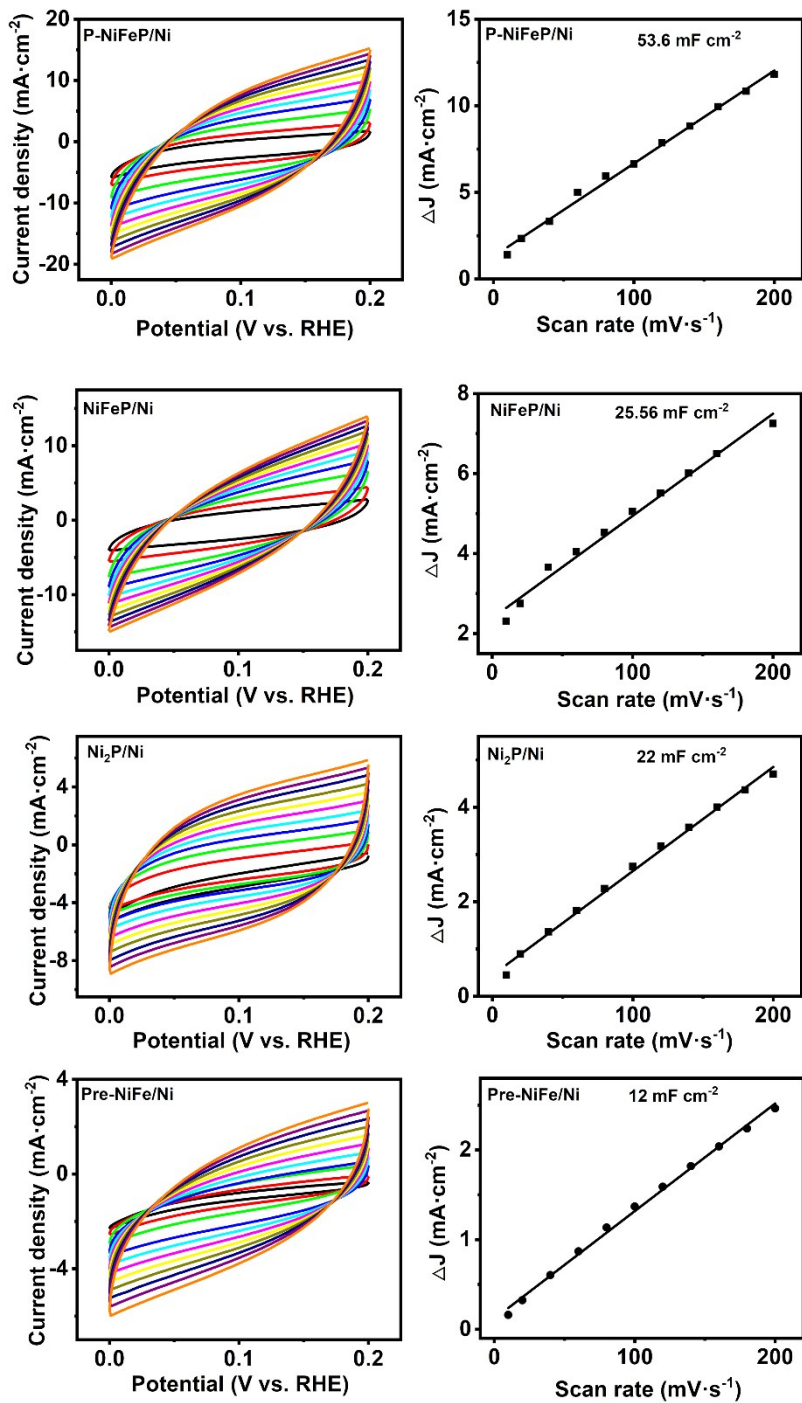


Fig. S7 The CV curves for catalysts with scanning rates from 10 to 200 mV s⁻¹ and the capacitive current densities as a function of scan rate for catalysts.

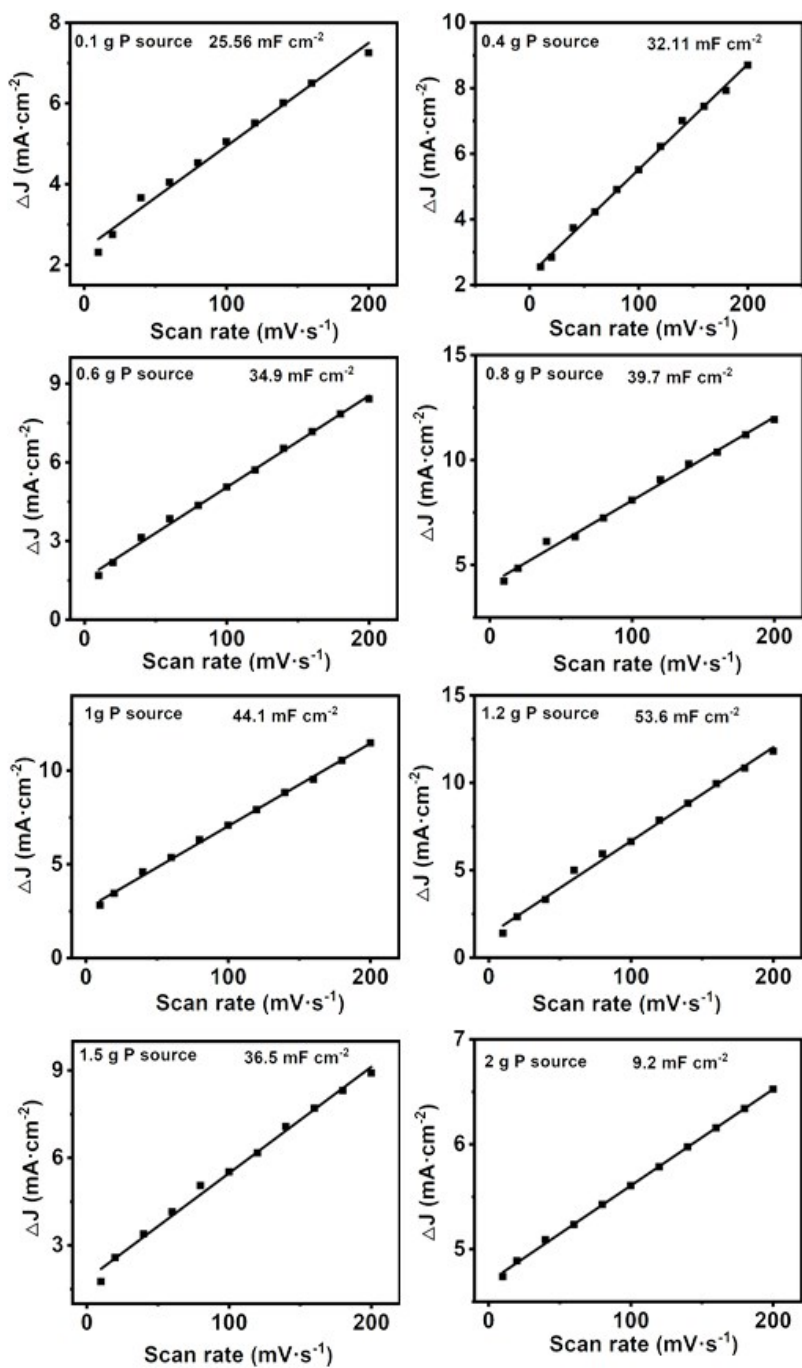


Fig. S8 The capacitive current densities as a function of scan rate for P-NiFeP/Ni with different phosphorus sources.

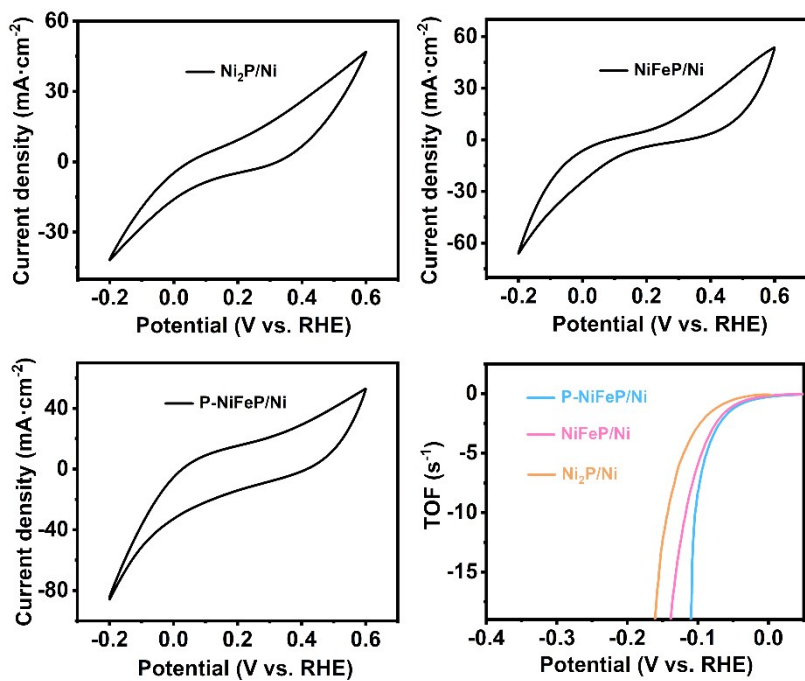


Fig. S9 The CVs with a scan rate of 100 mV s⁻¹ at pH=7 and turnover frequency for as-synthesized samples.

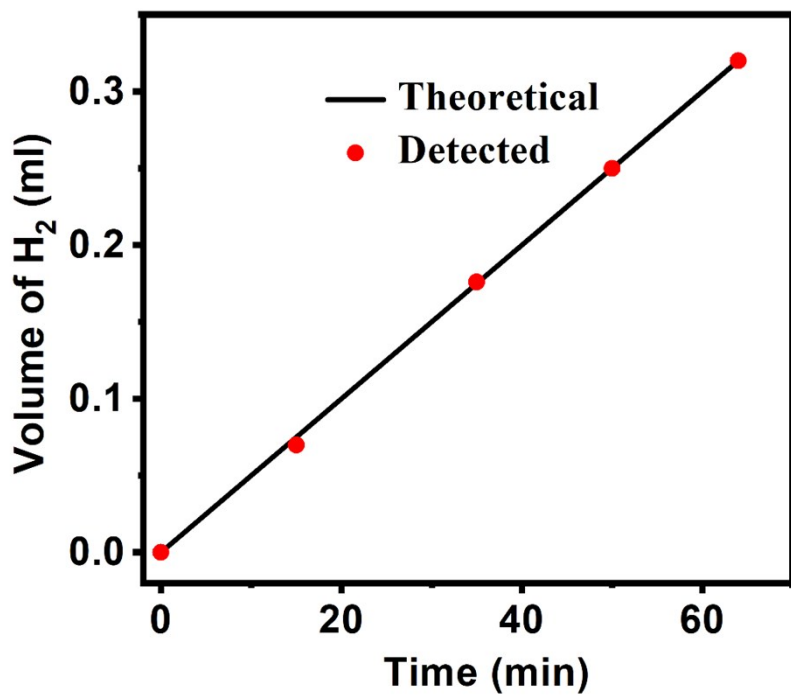


Fig. S10 The amount of H₂ theoretically calculated and experimentally measured versus time for P-NiFeP/Ni at pH = 14 at an overpotential of 300 mV for 80 min.

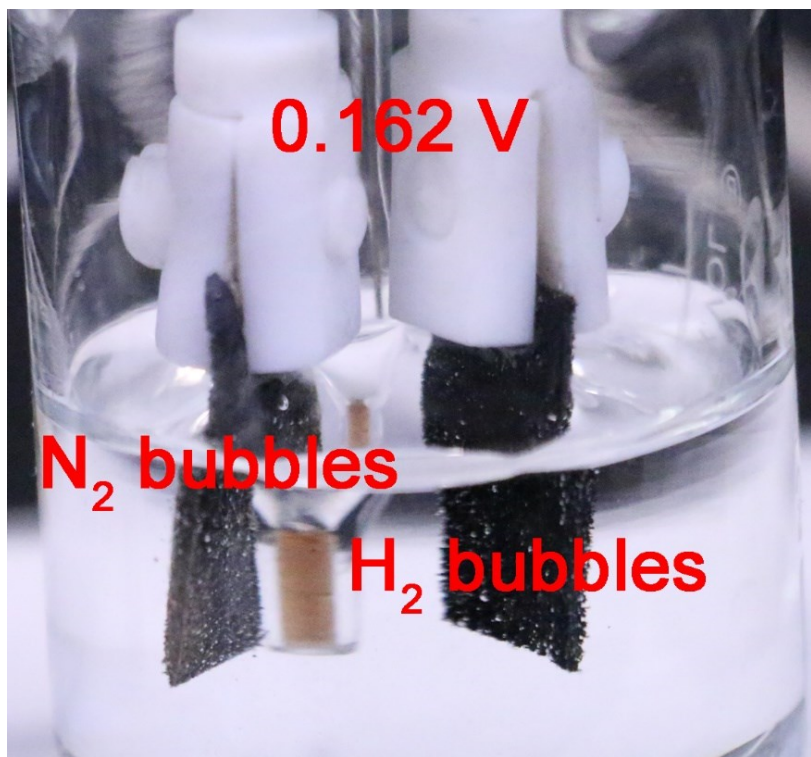


Fig. S11 The photo of the P-NiFeP/Ni electrode couple system for overall hydrazine splitting at 0.162 V voltage.

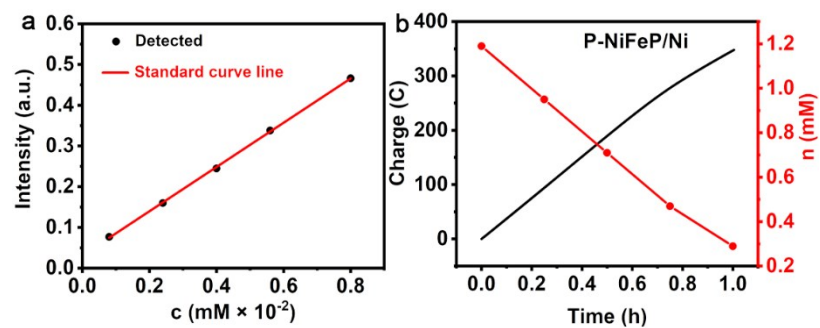


Fig. S12 (a) Calibration curve of reaction products of hydrazine with p-dimethylaminobenzaldehyde. (b) Hydrazine concentration–time and charge–time curve during constant potential (0.28 V vs. RHE) electrolysis.

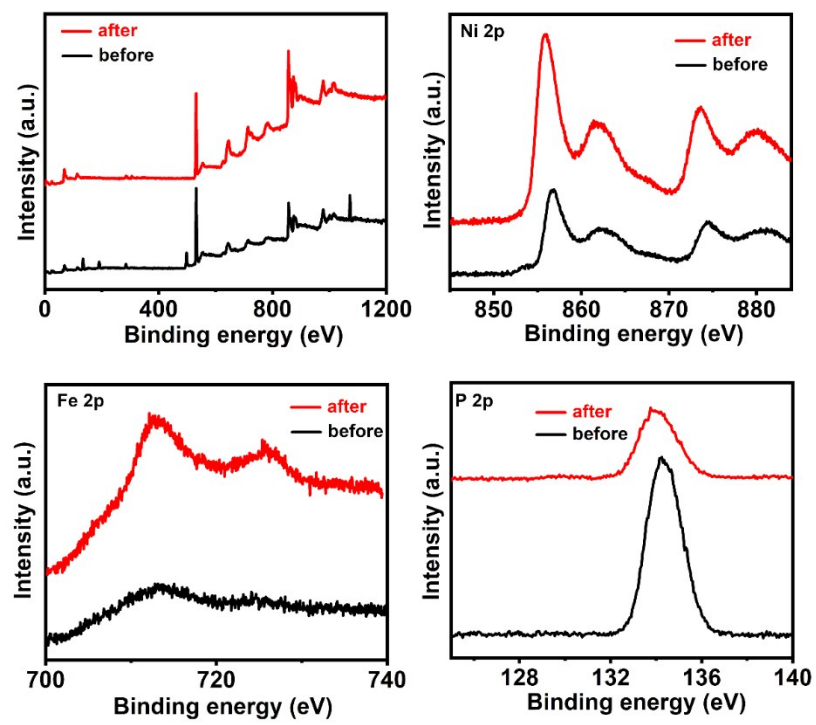


Fig. S13 The comparison of the XPS spectra of P-NiFeP/Ni before and after hydrazine oxidation.

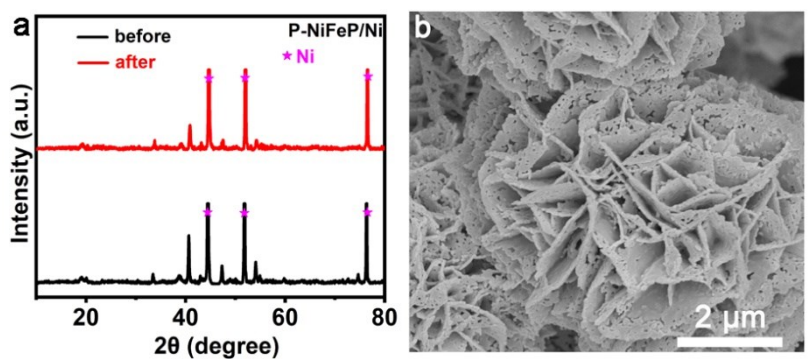


Fig. S14 The XRD pattern and SEM image of P-NiFeP/Ni after H₂OR.

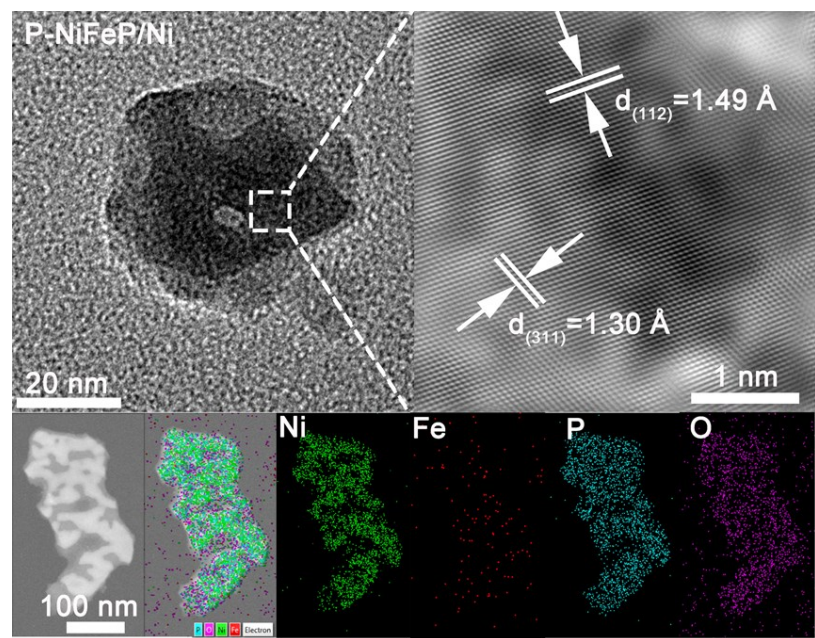


Fig. S15 The TEM image and corresponding the elements mapping of P-NiFeP/Ni after H₂OR.

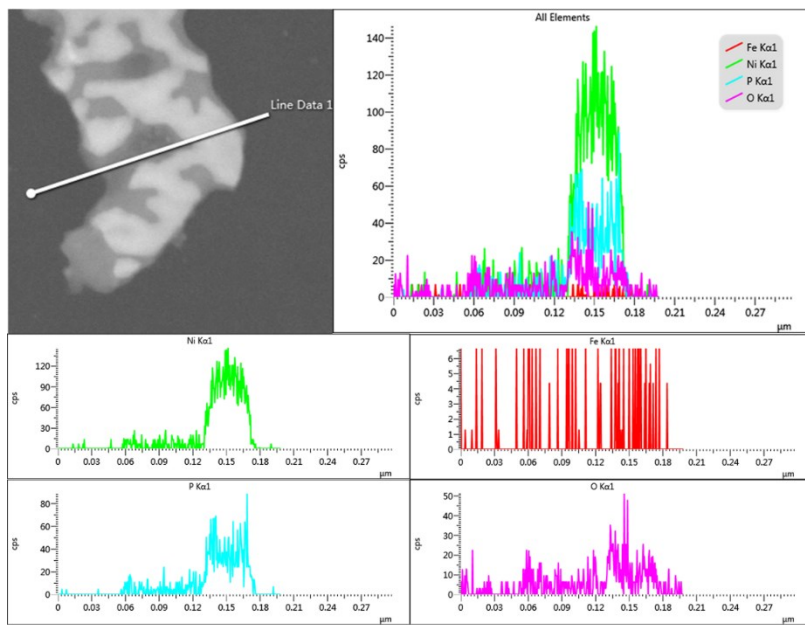


Fig. S16 The compositional line profiles of Ni (green), Fe (red), P (cyan), and O (pink) were recorded along the arrow of the sample after testing.

Table S1. The content of each element in P-NiFeP/Ni determined by XPS.

Element	Atomic (%)
C	9.65
O	58.26
Fe	4.87
Ni	12.8

P	14.42
---	-------

Table S2. The content of each element in P-NiFeP/Ni determined by EDS.

Element	Weight (%)	Atomic (%)
C	3.54	11.07
O	13.31	31.26
P	10.46	12.69
Fe	5.18	3.49
Ni	63.70	40.77
Pt	3.82	0.74

Table S3. Comparison of the HER performance of this work with the reported catalysts in 1.0 M KOH.

Materials	η_{10} (mV)	Tafle slope (mV dec ⁻¹)	Reference
P-NiFeP/Ni	17.9	63	This work
PW-Co ₃ N NWA/NF	41	40	1
Ni ₃ N/C	64	48	2

N-CoP ₂	38	46	3
Co ₂ N/Co	12	41.6	4
Co ₄ N	37	44	5
Co-Ni ₃ N	194	156	6
NiP ₂ -650	134	67	7
TM-ReSe ₂	109	81	8
SGNC-900	32	39	9

Table S4. Comparison of the H₂OR performance of this work with recently reported catalysts in 1.0 M KOH.

Catalysts	Current density (mA)	Overpotential (mV)	Reference
P-NiFeP/Ni	10	77	This work
	100	153	
	300	269	
	10	164	
CoSe ₂	50	96.9	10
Cu ₁ Ni ₂ -N	172	100	11
Ni _x P/NF	100	415	12
Ni ₃ S ₂ /NF	320	600	13
NiZn	40	600	14
NiCoSe ₂ /NF	75	600	15
Ni ₃ Se ₄ /NF	200	400	16
NiFeP/NM	300	300	17
Ni _{0.6} Co _{0.4} Se/NF	300	400	18

Notes and references

1 Y. Liu, J. Zhang, Y. Li, Q. Qian, Z. Li, Y. Zhu and G. Zhang, *Nat. Commun.*, 2020, **11**, 1853.

- 2 W. Ni, A. Krammer, C. S. Hsu, H. M. Chen, A. Schuler and X. Hu, *Angew. Chem., Int. Ed.*, 2019, **58**, 7445-7449.
- 3 J. Y. Cai, Y. Song, Y. P. Zang, S. W. Niu, Y. S. Wu, Y. F. Xie, X. S. Zheng, Y. Liu, Y. Lin, X. J. Liu, G. M. Wang and Y. T. Qian, *Sci. Adv.*, 2020, **6**, eaaw8113.
- 4 F. Song, W. Li, J. Yang, G. Han, T. Yan, X. Liu, Y. Rao, P. Liao, Z. Cao and Y. Sun, *ACS Energy Lett.*, 2019, **4**, 1594-1601.
- 5 Z. Chen, Y. Song, J. Cai, X. Zheng, D. Han, Y. Wu, Y. Zang, S. Niu, Y. Liu, J. Zhu, X. Liu and G. Wang, *Angew. Chem., Int. Ed.*, 2018, **57**, 5076-5080.
- 6 C. Zhu, A. L. Wang, W. Xiao, D. Chao, X. Zhang, N. H. Tiep, S. Chen, J. Kang, X. Wang, J. Ding, J. Wang, H. Zhang and H. J. Fan, *Adv. Mater.*, 2018, **30**, 1705516.
- 7 Q. Fu, X. Wang, J. Han, J. Zhong, Z. Tongrui, T. Yao, C. Xu, T. Gao, S. Xi, C. Liang, L. Xu, P. Xu and B. Song, *Angew. Chem., Int. Ed.*, 2020, **59**, 2-10.
- 8 I. S. Kwon, I. H. Kwak, S. Ju, S. Kang, S. Han, Y. C. Park, J. Park and J. Park, *ACS Nano*, 2020, **14**, 12184-12194.
- 9 R. Wei, Y. Gu, L. Zou, B. Xi, Y. Zhao, Y. Ma, Y. Qian, S. Xiong and Q. Xu, *Nano Lett.*, 2020, **20**, 7342-7349.
- 10 J. Y. Zhang, H. Wang, Y. Tian, Y. Yan, Q. Xue, T. He, H. Liu, C. Wang, Y. Chen and B. Y. Xia, *Angew. Chem., Int. Ed.*, 2018, **57**, 7649-7653.
- 11 Z. Wang, L. Xu, F. Huang, L. Qu, J. Li, K. A. Owusu, Z. Liu, Z. Lin, B. Xiang, X. Liu, K. Zhao, X. Liao, W. Yang, Y. B. Cheng and L. Mai, *Adv. Energy Mater.*, 2019, **9**, 1900390.
- 12 H. Wen, L. Y. Gan, H.-B. Dai, X. P. Wen, L. S. Wu, H. Wu and P. Wang, *Appl. Catal., B*, 2019, **241**, 292-298.

- 13 G. Liu, Z. Sun, X. Zhang, H. Wang, G. Wang, X. Wu, H. Zhang and H. Zhao, *J. Mater. Chem. A*, 2018, **6**, 19201-19209.
- 14 A. Serov, M. Padilla, A. J. Roy, P. Atanassov, T. Sakamoto, K. Asazawa and H. Tanaka, *Angew. Chem., Int. Ed.*, 2014, **53**, 10336-10339.
- 15 K. Akbar, J. H. Jeon, M. Kim, J. Jeong, Y. Yi and S. H. Chun, *ACS Sustain. Chem. Eng.*, 2018, **6**, 7735-7742.
- 16 J. Y. Zhang, X. Tian, T. He, S. Zaman, M. Miao, Y. Yan, K. Qi, Z. Dong, H. Liu and B. Y. Xia, *J. Mater. Chem. A*, 2018, **6**, 15653-15658.
- 17 Q. Sun, M. Zhou, Y. Shen, L. Wang, Y. Ma, Y. Li, X. Bo, Z. Wang and C. Zhao, *J. Catal.*, 2019, **373**, 180-189.
- 18 Z. Feng, E. Wang, S. Huang and J. Liu, *Nanoscale*, 2020, **12**, 4426-4434.